

REPORT DOCUMENTATION PAGE				Form Approved OMB No. 0704-0188	
The public reporting burden for this collection of information is estimated to average 1 hour per response, including the time for reviewing instructions, searching existing data sources, gathering and maintaining the data needed, and completing and reviewing the collection of information. Send comments regarding this burden estimate or any other aspect of this collection of information, including suggestions for reducing the burden, to Department of Defense, Washington Headquarters Services, Directorate for Information Operations and Reports (0704-0188), 1215 Jefferson Davis Highway, Suite 1204, Arlington, VA 22202-4302. Respondents should be aware that notwithstanding any other provision of law, no person shall be subject to any penalty for failing to comply with a collection of information if it does not display a currently valid OMB control number. <b>PLEASE DO NOT RETURN YOUR FORM TO THE ABOVE ADDRESS.</b>					
1. REPORT DATE (DD-MM-YYYY) 14-08-2015		2. REPORT TYPE Final		3. DATES COVERED (From - To) 25 Mar 2013 – 24 Mar 2015	
4. TITLE AND SUBTITLE  Realization of high-temperature superconductivity in nano-carbon materials and its application II			5a. CONTRACT NUMBER FA2386-13-1-4059		
			5b. GRANT NUMBER Grant 13RSZ067_134059		
			5c. PROGRAM ELEMENT NUMBER 61102F		
6. AUTHOR(S)  Assoc.Prof Junji Haruyama			5d. PROJECT NUMBER		
			5e. TASK NUMBER		
			5f. WORK UNIT NUMBER		
7. PERFORMING ORGANIZATION NAME(S) AND ADDRESS(ES) Aoyama Gakuin University 5-10-1 Fuchinobe, Sagamihara Kanagawa 229-8558 Japan			8. PERFORMING ORGANIZATION REPORT NUMBER  N/A		
9. SPONSORING/MONITORING AGENCY NAME(S) AND ADDRESS(ES)  AOARD UNIT 45002 APO AP 96338-5002			10. SPONSOR/MONITOR'S ACRONYM(S)  AOARD		
			11. SPONSOR/MONITOR'S REPORT NUMBER(S) 13RSZ067_134059		
12. DISTRIBUTION/AVAILABILITY STATEMENT  Distribution Code A: Approved for public release, distribution is unlimited.					
13. SUPPLEMENTARY NOTES					
14. ABSTRACT Superconductivity (SC) is one of the hottest topics in condensed matter physics and also for application to zero-emission energy system. In particular, carbon-based superconductors have attracted significant attention for high transition temperature ( $T_c$ ). The present work attempts to realize high- $T_c$ SC in thin films of carbon nanotubes (CNTs) by using ionic-gel (liquid) gating. Extremely high carrier density in CNT films caused by the optimized ionic-gel gate allows possible $T_c$ as high as 48K, while reproducibility is poor due to non-uniform ionization in the gel. In contrast, reproducible abrupt-resistance drop at $T \sim 47K$ is observed by ionic-liquid gating, whereas magnitude of the drop is small, but further optimization promises high- $T_c$ SC. On the other hand, edge spin of graphene can be also a good candidate for causing SC. Applying ionic-liquid gate voltage to graphene nanomesh (GNM) allows reconfirmation of induced polarized-spins at pore edges with anti-ferromagnetic (AFM) spin alignment. Moreover, tunnel magnetoresistance structure fabricated utilizing ferromagnetic GNM reveals that AFM alignment between pore-edge spins and spins of Co electrode is possible. AFM spin alignment promises possible SC based on graphene edge spins					
15. SUBJECT TERMS  Carbon nano tubes, Superconducting Materials					
16. SECURITY CLASSIFICATION OF:			17. LIMITATION OF ABSTRACT	18. NUMBER OF PAGES	19a. NAME OF RESPONSIBLE PERSON
a. REPORT	b. ABSTRACT	c. THIS PAGE			Ingrid J. Wysong, Ph.D.
U	U	U	SAR	10	19b. TELEPHONE NUMBER (Include area code) +81-42-511-2000

**“Realization of high-temperature superconductivity in nano-carbon materials and its application”**

Date: 07/13/2015

**Name of Principal Investigators (PI and Co-PIs): Junji Haruyama**

- e-mail address : J-haru@ee.aoyama.ac.jp
- Institution : Aoyama Gakuin University
- Mailing Address : 5-10-1 Fuchinobe, Chuo-ku, Sagamihara, Kanagawa 252-5258 Japan
- Phone : +81-42759-6256
- Fax : +81-42759-6256

Period of Performance: 03/25/2013 - 03/24/2015

**Abstract:** Superconductivity (SC) is one of the hottest topics in condensed matter physics and also for application to zero-emission energy system. In particular, carbon-based superconductors have attracted significant attention for high transition temperature ( $T_c$ ). In the present work, I have tried to realize high- $T_c$  SC in thin films of carbon nanotubes (CNTs) by using ionic-gel(liquid) gating. Extremely high carrier density in CNT films caused by the optimized ionic-gel gate allows possible  $T_c$  as high as 48K, while reproducibility is poor due to non-uniform ionization in the gel. In contrast, reproducible abrupt-resistance drop at  $T \sim 47K$  is observed by ionic-liquid gating, whereas magnitude of the drop is small, but further optimization promises high- $T_c$  SC. On the other hand, edge spin of graphene can be also a good candidate for causing SC. Applying ionic-liquid gate voltage to graphene nanomesh (GNM) allows reconfirmation of induced polarized-spins at pore edges with anti-ferromagnetic (AFM) spin alignment. Moreover, tunnel magnetoresistance structure fabricated utilizing ferromagnetic GNM reveals that AFM alignment between pore-edge spins and spins of Co electrode is possible. These AFM spin alignment promises possible SC based on graphene edge spins.

**(1) Introduction:**

**High- $T_c$  SC in CNTs thin films with ionic gel and liquid gates:**

For 2004 – 2008, there was significant advancement of carbon-based SC materials, such as highly boron-doped diamond with  $T_c \sim 4K - 10K$ , Calcium (Ca)-intercalated graphite ( $CaC_{60}$ ) with  $T_c \sim 12 - 15K$ , two-different types of CNTs with  $T_c \sim 12- 19K$ , and pressure-applied cesium-doped fullerene ( $Cs_3C_{60}$ ) with  $T_c \sim 38K$ . The issue based on CNTs was realized by my group as follows; (1) SC in entirely end-bonded multi-walled CNTs (MWNTs) with the world-highest  $T_c$  of 12K and (2) SC in thin films consisting of boron-doped single-walled CNTs (SWNTs) with  $T_c = 12-19 K$ . CNTs should, however, provide much higher  $T_c$ , which originates from high phonon-frequency of carbon atoms, extremely high electronic density of states (EDOSs) in van Hove singularities (VHSs) of one-dimensional conductor, and strong electron-phonon coupling between radial breathing phonon mode and  $\sigma$ - $\pi$  electrons. Based on these factors, even  $T_c$  as high as 64K was theoretically predicted by Harvard group. However, how to highly dope carriers for high- $T_c$  SC still remain as the most important problem.

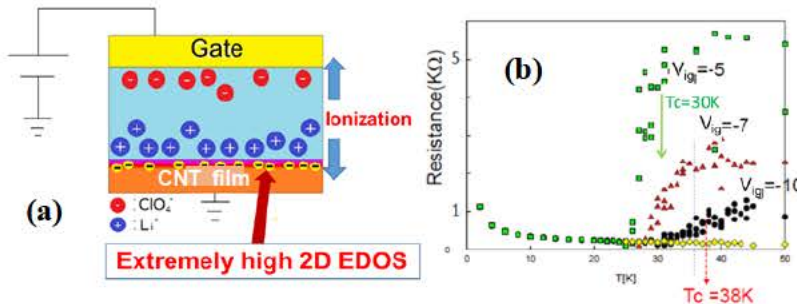


**Fig. 1** (a) Schematic cross-sectional view of ionic gel gating on CNT film. (b) High- $T_c$  (38K) SC observed in ionic-liquid gel gated CNT thin film found in 2014.

On the other hand, an ionic-gel (liquid) gating method is actively used in recent some materials. Because applying ionic-gel (liquid) gating voltages causes extremely high EDOS (i.e., carriers) on the

sample surface through ionization and subsequently formation of electrical double layer (Fig. 1(a)), the high EDOS has caused SC even in insulators. In last year, I have tried to realize high- $T_c$  SC in thin films of SWNTs employing this ionic-gel gating method. Then, I found a high possibility of high- $T_c$  SC with  $T_c$  as high as 38 K (Fig. 1(b)). However, reproducibility, which is one of the most important scientific factors for SC, was quite poor. Only a few samples showed this high  $T_c$ . The main reason was poor uniformity of ionization due to poor uniformity of ionic ion ( $\text{LiClO}_4$ ) mixed into hard gel structure.

Thus, in the present work, (1) I have tried to optimize the component of ionic gel consisting of  $\text{LiClO}_4$ , poly-ethylene oxide (POE), and water. Moreover, (2) I have also tried to employ ionic liquid gate (DEME-TFSI), which does not have this problem and has much higher efficiency of ionization.

### Graphene nanomesh spintronics for SC

As the other novel material, two-dimensional (2D) mono-atomic layers are attracting significant attention. Graphene, which is a 2D mono-atomic layer of graphite, triggered this active research by developing mechanical exfoliation method of graphite using scotch tape leading to Nobel Prize at 2010. Among those, edge-based phenomena are interesting. A specified edge atomic structure (the so-called zigzag-type edge) of graphene produces a flat energy band, resulting in strong electron localization and emergence of spontaneous spin polarization. It is highly expected that the polarized spins can produce SC, if the spin alignment would become anti-ferromagnetic and Cooper pairs would be formed, although none reported on SC in graphenes. Thus, we have fabricated novel edge system of graphenes (i.e., Fig. 2(a); low-defect GNMs with honeycomb like array of hexagonal nanopores, which were fabricated by non-lithographic method) and explored SC by terminating the pore edge by foreign atoms (e.g., hydrogen (H), oxygen, boron).

In 2014, we reported that H-terminated zigzag-type pore edges of GNMs can yield spontaneously polarized electron spins and flat-band ferromagnetism. The magnitude of ferromagnetism in the ferromagnetic GNMs (FGNMs) was small (e.g.,  $\sim 10^{-6}$  emu/ $\text{mm}^2$ ) owing to the small area of the mono-H-termination of zigzag pore edges, because H-termination was only performed using critical-temperature annealing under  $\text{H}_2$  atmosphere. In contrast, I significantly improved the ferromagnetism amplitude ( $> \sim 100$  times) even at room temperature by controlling mono-H-termination using HSQ resist treatment with electron beam (EB) irradiation (Fig. 2(b, c)). The mono-H-termination of pore edges could be realized using EB irradiation to the HSQ resist. The HSQ resist ( $\text{HSiO}_{3/2}$ ) $_n$  consisted of H, Si, and O atoms. The atomic bonds related to H (i.e., H-Si and H-O bonds) were easily detached by EB irradiation, and atomic H species could be produced from the HSQ resist because the binding energy of H-Si was  $\sim 3$  eV, whereas EB irradiation energy was larger than 1 KeV even at the smallest case. The excess dose depending on irradiation time could form C-H bonds with a binding energy of  $\sim 2.2$  eV and the mono-H termination of the zigzag pore edges by the detached H-atoms in the large area of GNMs. Because only mono-H-termination of zigzag edges can produce a large flat-band ferromagnetism, this could result in a large-amplitude ferromagnetism.

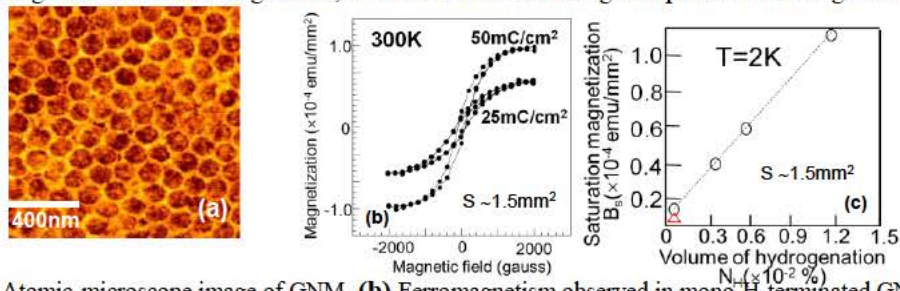


**Fig. 2** (a) Atomic-microscope image of GNM. (b) Ferromagnetism observed in mono-H-terminated GNM with zigzag-type pore edges. The mono-H-termination was realized using HSQ resist treatment with EB irradiation. (c) Magnetization vs. hydrogenation volume, realized by HSQ resist treatment. Red triangle shows the case of non-HSQ resist treatment.

In order to reconfirm presence of edge polarized spins and spin interaction for causing high- $T_c$  SC, in the present work, I have carried out the following two experiments; (1) Observation of EDOS of the pore edges by using ionic liquid and (2) formation of tunnel magnetoresistance (TMR) structure.

## Experiments: Sample fabrications

### (1) High-Tc SC in CNTs thin films with ionic gel and liquid gates:

I have synthesized two-type of CNTs; i.e., metallic and semiconductive electronic behaviors. Then, thin films consisting of only individual CNT have been fabricated. To realize highly uniform and densely thin films, a large amount of purified CNTs have been deposited on Si substrate by using spin coater with the optimized substrate rotation speed.

Then, ionic gel has been deposited on the CNT thin films (Fig. 3(a)). In order to optimize component of ionic gel, weight of  $\text{LiClO}_4$ , POE, and water volume have been precisely arranged (Table. 1).  $\text{LiClO}_4$  has been mixed into PEO with using water. Samples S1-3 are basic structure. For S4-6 and S7-9, only weight of PEO has been changed. For S10-12, water volume has been also changed. Annealing temperature for these ionic gel was also optimized. Then, I explored high-Tc SC with high reproducibility by measuring temperature dependence of resistivity of individual samples.

Sample No	Weight of $\text{LiClO}_4$ ion [mg]	PEO [mg]	Water [ $\mu\text{L}$ ]
S-1	22.45(1.5)	5	30
S-2	15.3(1)	5	30
S-3	7.15(0.5)	5	30
S-4	22.45(1.5)	2.5	30
S-5	15.3(1)	2.5	30
S-6	7.15(0.5)	2.5	30
S-7	22.45(1.5)	7.5	30
S-8	15.3(1)	7.5	30
S-9	7.15(0.5)	7.5	30
S-10	22.45(1.5)	5	50
S-11	15.3(1)	5	50
S-12	7.15(0.5)	5	50
S-13	22.45(1.5)	7.5	50
S-14	15.3(1)	7.5	50
S-15	7.15(0.5)	7.5	50

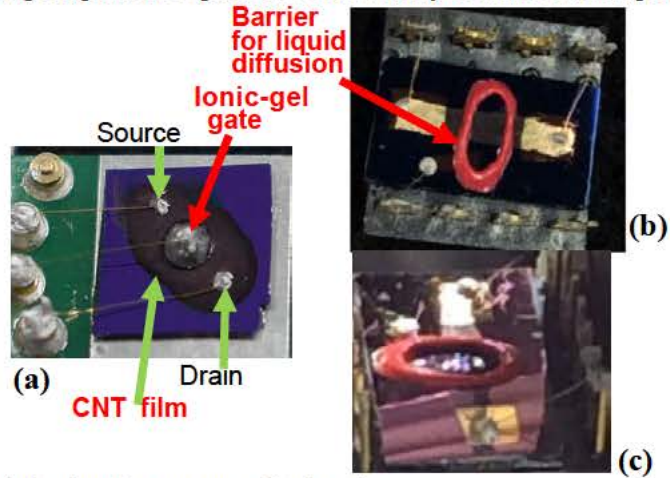


**Table 1:** Sample structures used for optimization of components of ionic gel.

**Fig. 3 (a)** Optical microscope top-view of CNT thin film FET with ionic gel gate. Two probe measurement has been employed just to detect resistance drop due to SC. **(b)(c)** Optical microscope views of CNT thin film FETs with ionic liquid gate. The red circle in (b) is the barrier block to enclose ionic liquid. It effectively blocks diffusion of ionic liquid to Au electrodes. Applied side-gate voltage causes ionization in the liquid and then extremely high DOS on surface of CNT film (Fig. 1(a)). In (c), sample holder has been improved parallel to ground to avoid dropping of the liquid for measurements.

Moreover, I have employed ionic liquid instead of ionic gel (Fig. 3(b)(c)), because it can resolve the problem of ionic gel about non-uniform ionization, which is explained in experimental result, and also it is known that ionic liquid gate has much higher efficiency for causing high EDOS on sample surface. For this, I had to improve measurement system for sample attachment. Ionic liquid has to be placed perpendicular to ground on the CNT film substrate, because it drops from the sample surface by gravity. Thus, sample holder of low-temperature measurement system has been improved so as to be parallel with ground (Fig. 3(c)). Furthermore, the ionic liquid quickly diffuses through space among CNTs in the film structure. This situation is very different from conventional materials without including any spaces. Diffused liquid quickly attains to two metal (Au) electrodes and electric features become just short (i.e., low resistance). Thus, I have fabricated a barrier to protect this liquid diffusion on sample surface and dropped ionic liquid inside of the barrier. Diffusion of the liquid has been drastically improved by this structure.

### (2) Graphene nanomesh spintronics for SC

To realize SC in graphene, I have utilized polarized spins of edges of graphene. Graphene nanomesh (GNM), consisting of honeycomb-like array of hexagonal nanopores, has a large amount of edges at the nanopores. H-terminated GNM shows polarized edge spins and ferromagnetism. In order to reconfirm presence of edge polarized spins and spin interaction, I have carried out the following two experiments in this time; (1) Observation of EDOS of the pore edges by using ionic liquid gate and (2) formation of tunnel magnetoresistance (TMR) structure and observation of TMR behaviors.

Figure 4(a) shows optical microscope image of the ionic liquid on GNM-FET. The ionic liquid was placed between side gate and current channel of the GNM FET. The applied side-gate voltage as ionic-liquid gate voltage causes ionization and strong electrical field on the pore edges. This induces EDOS of the pore edges and allows observation of EDOS at pore edges.

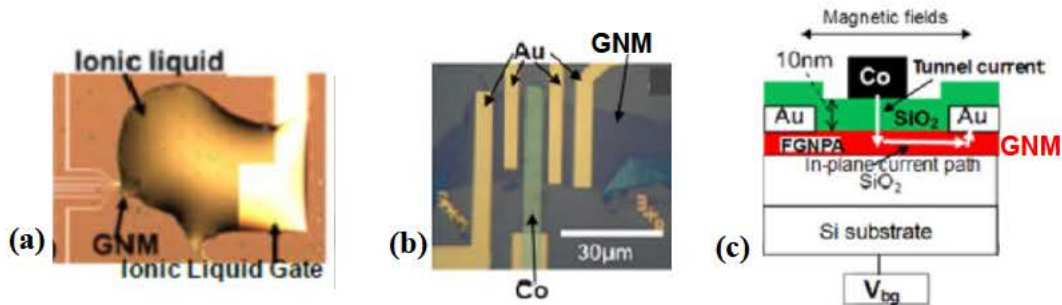


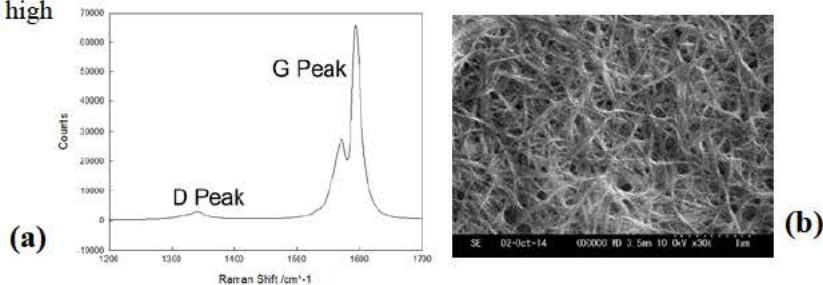
**Fig. 4** (a) Optical-microscope top-view of GNM with ionic liquid gate (DEME-1FSI). (b) Optical-microscope top-view and (c) schematic cross-sectional view of TMR structure, consisting of ferromagnetic-GNM/SiO<sub>2</sub> tunnel barrier/Co electrode.

Figures 4(b)(c) show optical microscope top-view (b) and schematic cross-sectional view (c) of the TMR structure, which consists of ferromagnetic GNM/SiO<sub>2</sub> tunnel-barrier/Co electrode. Polarized pore-edge spins of GNM tunnel through SiO<sub>2</sub> layer and interact with polarized spins in Co electrode.

**Results and Discussion:**

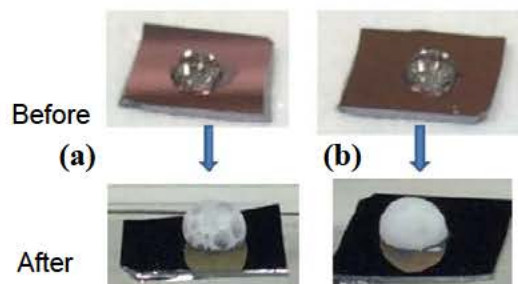
**(1) High-T<sub>c</sub> SC in CNTs thin films with ionic gel and liquid gates:**

Figure 5(a) shows observed typical Raman spectrum of CNT thin film (Fig. 5(b)). It shows clear G-peak, which suggests high quality of the CNTs. It also shows almost zero D-peak height, which suggests absence of defects and impurities. Consequently, it is reconfirmed that quality of the CNT film is quite high



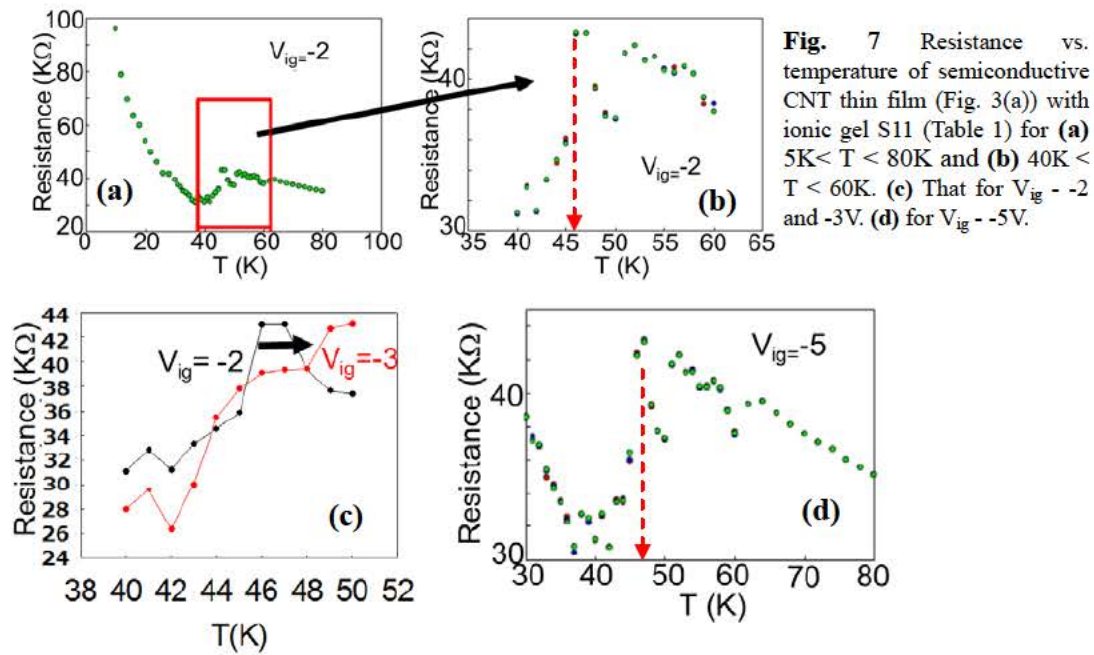
**Fig. 5** (a) Typical Raman spectrum of CNT thin film (b). (b) SEM top-view of CNT thin film.

Figure 6 shows optical microscope view of ionic gels before and after annealing at 110 °C. In order to exclude impurity gas and obtain high quality ionic gel, I have carried out this annealing. After the annealing, color of the gels changes from transparency to white, because water and impurity gas evaporate. This also means that the gel becomes much harder state.



**Fig. 6** Examples of optical microscope images of ionic gels before and after annealing for (a) S2 and (b) S11 in Table 1.

Figure 7 shows typical results of the observed high-T<sub>c</sub> SC in semiconducting CNT thin films with ionic-gel gating using condition S11 in Table 1. An abrupt resistance drop at T<sub>c</sub> = 46 K is evidently observed under V<sub>ig</sub> = -2V (Fig. 7(a) and 7(b)), although the resistance increases at low temperature because of presence of contact resistance in the two-probe measurement. When V<sub>ig</sub> = -3V, the T<sub>c</sub> increases slightly with two-step resistance drops (Fig. 7(c)). At V<sub>ig</sub> = -5V, T<sub>c</sub> = 48K becomes more evident in Fig. 7(d). These T<sub>c</sub> are amazing, because they are higher than 40K. Only CuO<sub>2</sub>-based and Fe-based superconductors have previously shown T<sub>c</sub> > 40K among various superconductors. In particular, carbon-base new SC exhibited T<sub>c</sub> < 20K in any materials as explained in introduction (except for pressure-applied Cs<sub>3</sub>C<sub>60</sub> as a specified case). Therefore, if this T<sub>c</sub> = 48K would be highly reproducible, it must give a large impact to community.



**Fig. 7** Resistance vs. temperature of semiconductive CNT thin film (Fig. 3(a)) with ionic gel S11 (Table 1) for (a)  $5K < T < 80K$  and (b)  $40K < T < 60K$ . (c) That for  $V_{ig} = -2$  and  $-3V$ . (d) for  $V_{ig} = -5V$ .

However, reproducibility of this high- $T_c$  SC is still poor like the case of last year's SC with  $T_c$  of 38K as shown in introduction. Although I have optimized the gel condition (Table 1) and found that S11 is one of the best condition, the high  $T_c$  cannot yet be controlled even in it. Only three samples among 30 samples exhibited high  $T_c$  around 37K - 48K, depending on  $V_{ig}$ . The main reason of this poor reproducibility is how to mix the gel component and also annealing of gel. When I mix  $LiClO_4$  into POE with water,  $LiClO_4$  cannot be uniformly diffused into POE even with using a large volume of water (S10-15 in Table 1), because POE is in strong gel state. This leads to non-uniform ionization of  $LiClO_4$  in the POE and subsequently poor reproducibility of the high- $T_c$  SC. Moreover, I had to carry out annealing to exclude impurity gas from the ionic gel. This also leads to non-uniform ionization of  $LiClO_4$ , because water component decreased by the annealing and POE became harder.

Thus, in order to resolve this problem, I have employed ionic-liquid for the same CNT thin films instead of the ionic gel, because it does not use POE and hence ionization can be caused much more uniformly. It is also well known that ionization efficiency of the ionic liquid is higher than that in gel.

As an ionic liquid, I have selected DEME-TFSI in this experiment. Figure 8 shows one of the measurement results for abrupt resistance drop with  $T_c$  as high as 47K observed in metallic CNT thin films. This  $T_c$  is reproducible for 7 samples, while amplitude of the resistance drop is small even considering influence of two-probe measurements. This reason is due to insufficient optimization of the ionic liquid conditions. They are still under investigation. However, the high reproducibility is much different from the case of ionic gel gate. Therefore, one can strongly expect high  $T_c$  with high reproducibility in this system.

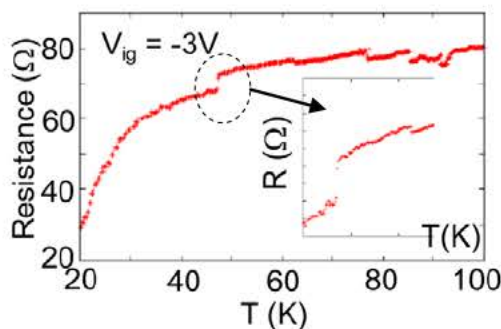


**Fig. 8** Resistance vs. temperature of metallic CNT thin film with ionic liquid gate (Fig. 3(b)(c): DEME-TFSI). Dotted circle means an abrupt resistance drop. Although the magnitude is small, it is highly reproducible. **Inset:** Expansion of resistance drop in main panel.

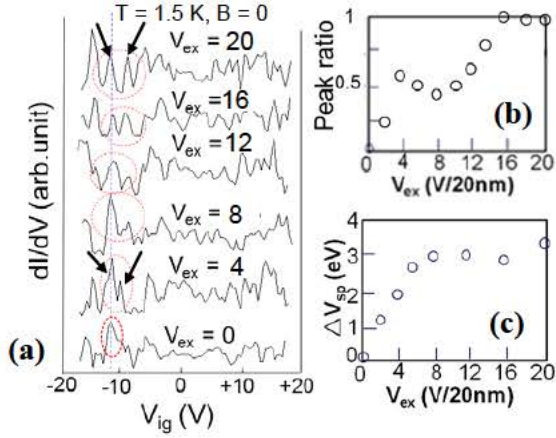
## (2) Graphene nanomesh spintronics for SC

### 1: Observation of EDOS of the pore edges by using ionic liquid

Zigzag-type atomic structure of the pore edges causes flat energy band and extremely high EDOS. Applying high electric field by using ionic liquid (DEME-TFSI) gating allows reconfirmation of this

EDOS via. induced EDOS. When large ionic liquid gate voltage ( $V_{ig}$ ) is applied,  $dI/dV$  maximum, which suggest possible presence of high EDOS, is observed around  $V_{ig} = \sim 13V$  at applied external voltage ( $V_{ex}$ ) of 0 V (red dotted circle in Fig. 9(a)). With increasing  $V_{ex}$ , this maximum peak splits to two peaks (shown by two arrows in Fig. 9(a)). The peak spacing  $V_{ex}$  increases with increasing  $V_{ex}$  to 8V, while it saturates above  $V_{ex} = 8V$  (Fig. 9(b)). The peak ratio of these two peaks (right/left peak heights in Fig. 9(a)) becomes 0.5 around  $V_{ex}= 8V$ , whereas it increases above 8V (Fig. 9(c)).

These behaviors of  $dI/dV$  can be well understood by presence of anti-ferromagnetic (AFM) spin moments at two edges of interpore graphene nanoribbon (GNR) region of the GNM. GNM consists of a large amount of hexagonal nanopores (Fig. 2(a)) and the interpore region can be a GNR, which is one-dimensional strip line of graphene. As explained in introduction, I have previously confirmed presence of polarized spins at the pore edges and, thus, the interpore GNR edges. Density of these



polarized spins is significantly induced by applied  $V_{ig}$ , corresponding to the  $dI/dV$  peak at  $V_{ex} = 0$ . When  $V_{ex}$  is applied, spin band gap increases, if spin configuration is AFM at two edges of a GNR. Figure 9(c) and 9(d) qualitatively suggests this. Consequently, I could reconfirm presence of AFM spins in the pore edges of GNM. This promises production of SC, because AFM spin configuration must lead to emergence of Cooper pairs.

**Fig. 9** (a) Differential conductivity ( $dI/dV$ ) as functions of  $V_{ig}$  and  $V_{ex}$  in GNM with ionic liquid gate (Fig. 4(a)). Red dotted circle means the maximum. (b) Voltage difference between two peaks shown by two arrows in (a). (c) Ratio of two peak heights in (a) (i.e., right/left peak heights).

## 2: Tunnel magnetoresistance (TMR) behaviors.

Figure 10 shows TMR ratio as a function of magnetic field (B) at (a)  $T = 2 K$  and (b) room temperature. Indeed, one can confirm presence of TMR ratio peaks, although the peak shape is not sharp but broad. Although TMR ratio peak of  $\sim 20\%$  at  $T = 2K$  is low, it is surprising that the peaks are observed even at room temperature because ferromagnetic GNM uses no ferromagnetic materials.

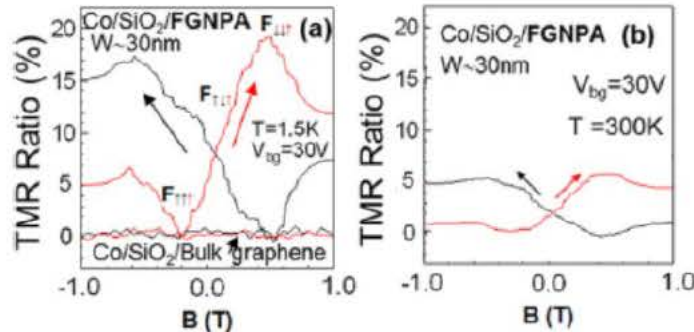


**Fig. 10** TMR ratio of Fig. 4 (b)(c) structure as a function of magnetic field (B) at (a)  $T = 2 K$  and (b) room temperature.

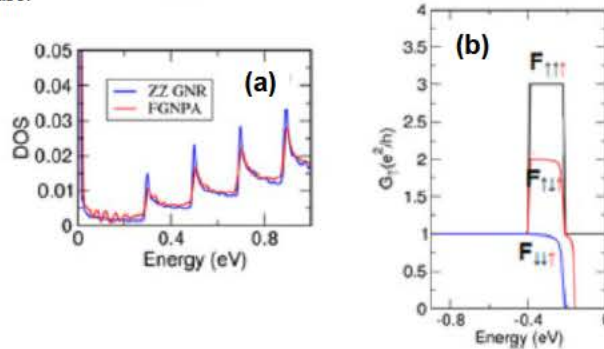


**Fig. 11** (a) DOS at edges as a function of energy for graphene nanoribbon (GNR) and GNM with zigzag edges. (b) Tunnel magnetoconductance (MC) for TMR structure shown in Fig. 4(b)(c). Arrows in subscript of "F" mean spin moments of two edges of interpore GNR (black two arrows) and that in Co electrode (red one arrow).

In order to confirm the origin of this TMR behavior, theoretical calculation has been carried out using first principal method. The results are shown in Fig. 11. Figure 11(a) exhibits DOS at edges as a function of energy for graphene nanoribbon (GNR) and GNM with zigzag edges. They actually show similar DOS, because the GNM consist of a large number of interpore GNRs (Fig. 2(a)). This suggests that theory of spin configuration for GNR edges can be applied also to GNM. Based on this, Fig. 11(b) shows tunnel magnetoconductance (MC) for TMR structure shown in Fig. 4(c). Indeed, three MC behaviors (i.e., MC maximum, minimum, and transition state) can be confirmed.

As shown by arrows, which mean spin moments, MC maximum appears when spin moments of two edges of an interpore GNR and spin moment of Co electrode are parallel (i.e., ferromagnetic (FM)), because this spin alignment makes spin scattering through the tunnel junction minimum. In contrast, MC minimum appears when they are anti-parallel (i.e., AFM), because of the spin scattering through the junction becomes maximum. In a transition regime between these two spin alignments, MC value becomes half of these two MC values, because only one of two edge spins of the interpore GNR becomes AFM. Consequently, these three states depending on B correspond to gradual change in the TMR ration as shown in Fig. 10(a). This result implies that polarized spins at pore edges actually exists in GNM and one can control the spin moment and its alignment, leading to appearance of SC. This result also promises realization of rare-magnetic material free spintronics.

### **Conclusion**

In conclusion, I tried to realize high- $T_c$  SC in thin films of CNTs by using ionic-gel(liquid) gating. Extremely high carrier density in CNT films caused by the optimized ionic-gel gate ( $\text{LiClO}_4+\text{PEO}$ ) allowed possible  $T_c$  as high as 48K, while the reproducibility was poor due to non-uniform ionization in the gel within a hard state even using large volume of water. In contrast, reproducible abrupt-resistance drop at  $T \sim 47\text{K}$  was observed by ionic-liquid gating (DEME-TFSI), whereas magnitude of the drop was small. However, the high reproducibility promises high- $T_c$  SC by further optimization of ionic liquid conditions.

On the other hand, applying ionic-liquid gate voltage to GNM allowed reconfirmation of the induced polarized-spins at the pore edges with AFM spin alignment. Moreover, TMR structure (ferromagnetic GNM/ $\text{SiO}_2$ -tunnel barrier/Co electrode) revealed that AFM alignment between the pore-edge spins and the spins of Co electrode was possible. These AFM spin alignment promises emergence of SC based on graphene edge spins.

## List of Publications and Significant Collaborations that resulted from your AOARD supported

**project:** In standard format showing authors, title, journal, issue, pages, and date, for each category list the following:

- a) papers published in peer-reviewed journals,
1. T. Hashimoto, S. Kamikawa, J. Haruyama, D. Soriano, J. G. Pedersen, S. Roche  
“Tunneling magnetoresistance phenomena utilizing graphene magnet electrodes”,  
Appl. Phys. Lett. 105, 183111 (2014)
  2. T. Kato, T. Nakamura, J. Kamijyo, T. Kobayashi, Y. Yagi, J. Haruyama,  
“High-Efficiency Graphene Nanomesh Magnets Realized by Controlling Hydrogenation of Pore Edges”, Appl. Phys. Lett. 104, 252410 (2014)
  3. J. Haruyama, “Superconductivity in carbon nanotubes”  
in “Carbon-based new superconductors; Toward high  $T_c$ ” edited by J. Haruyama  
(Pan Stanford Publishing, Singapore 2014/10/21) ISBN-10: 9814303305
  4. T. Hashimoto, S. Kamikawa, Y. Yagi, J. Haruyama,  
“Electronic Properties of Nanopore Edges of Ferromagnetic Graphene Nanomeshes at High Carrier Densities under Ionic-Liquid Gating”,  
Materials Sciences and Applications 5(1), 1-9 (2014)  
(Down loads in the first half year >> 800 times)
  5. S. Kamikawa, T. Shimizu, Y. Yagi, J. Haruyama,  
“Edge-sensitive semiconductive behaviors in low-defect narrow graphene nanoribbons”,  
Nanomaterials and Nanotechnology 4:12 | doi: 10.5772/58466 (2014)
  6. T. Hashimoto, S. Kamikawa, Y. Yagi, J. Haruyama, H. Yang, M. Chshiev,  
“Graphene edge spins: -Spintronics and Magnetism in graphene nanomeshes”,  
Nanosystems: Physics, Chemistry, Mathematics Journal 5(1), 25-38 (2014)
  7. J. Haruyama, “Graphene spintronics and magnetism”, in “The Graphene Optoelectronics. Synthesis, Characterization, Properties, and Applications” edited by Abd. Rashid bin Mohd Yusoff, Kyung Hee, WILEY-VCH Verlag (2014) ISBN: 978-3-527-33634-0
  8. K. Tada, N. Kosugi, K. Sakuramoto, T. Hashimoto, K. Takeuchi, Y. Yagi, J. Haruyama, H. Yang, M. Chshiev,  
“Electron-Spin-Based Phenomena Arising from Pore Edges of Graphene Nanomeshes”  
Journal of superconductivity and novel magnetisms, 26, 1037 (2013)
  9. J. Haruyama, “Graphene and Graphene Nanomesh Spintronics”,  
Special Issue on "Carbon Nanoelectronics" in Electronics, 2(4), 368-386 (2013)
- d) conference presentations without papers,
- Invited talks
1. “Hydrogenated graphene spintronics and magnetism”, International Conference on Advances in Functional Materials, New York, USA (June 2015)
  2. “Graphene spintronics”, International Conference and Exhibition on Mesoscopic & Condensed Matter Physics, Boston, USA (June 2015)
  3. “Graphene spintronics and magnetism”, World Congress and Expo on Nanotechnology and Materials Science, Dubai, UAE (April 2015)
  4. “Graphene and graphene nanomesh spintronics”, The 9th international conference on surfaces, coatings, and nanostructured materials, Dublin, Ireland (September 2014)
  5. “Self-assembled graphene nanomesh spintronics and magnetism”, The 5th international conference on Nanostructures self-assembly, Marseille, France (July 2014)
  6. “Graphene spintronics as topological insulator”, Graphene Week 2014 – The 8th International Conference on the Fundamental Science of Graphene and Applications of Graphene-Based Devices, Gothenburg, Sweden (June 2014)
  7. “Topological insulator, spintronics, and magnetism in graphenes”, International Conference on Superconductivity and Magnetism, Antalya, Turkey (April 2014)
  8. “Graphene spintronics and magnetism”,  
International conference on Small Science, Las Vegas, USA (December 2013)
  9. “Graphene spintronic and magnetic devices”, The 17th International workshop on the Physics of Semiconductor Devices, Noida, India (December 2013)

10. "Spin-based phenomena in graphenes",  
The 3rd Annual World Congress of Nano-Science & Technology, China (October, 2013)
  11. "Graphene spintronics", International conference on Nanoscale Magnetism,  
Istanbul, Turkey (September 2013)
  12. "Spintronics, magnetism, and superconductivity in graphenes and carbon nanotubes", University  
College London, Seminar (August 2013)
  13. "Graphene spintronics on graphene edges",  
International conference on Advanced Carbon Nanostructures, St.Petersberg, Russia(July 2013)
  14. "Research of high- $T_c$  superconductivity in carbon nanotubes", The 14th International  
conference on the Science and Applications of Nanotubes, Espoo, Finland (June 2013)
- e) manuscripts submitted but not yet published,
1. Y. Katagiri, T. Nakamura, C. Ohata, J.Haruyama et al.,  
"Atomically-thin molecular Schottky junction on electron-beam irradiated few-layer  $\text{MoS}_2$ ",  
Nature Nanotech. In-depth-review (<http://www.ee.aoyama.ac.jp/haru-lab/>)
  2. Y. Nakanishi, C. Ohata, J.Haruyama et al.,  
"Colossal edge magnetism in oxidized few-layer black phosphorous nanomesh",  
Nature Commun. In-depth-review (<http://www.ee.aoyama.ac.jp/haru-lab/>)
  3. K. Kamijo, T. Nakamura, J. Haruyama et al.,  
"Suppression of dephasing by spin-orbit-interaction in slightly hydrogenated graphenes",  
Nature Commun. In-depth-review (<http://www.ee.aoyama.ac.jp/haru-lab/>)
  4. J.Haruyama, "Magneism and spintronics in Graphenes"  
in "Recent advancement of Graphenes", American Nano Society In press
  5. J.Haruyama, "Nanomagnetism derived from graphene edge spins"  
in "Nanomagnetism", One Central Press (UK) In press